Crustal Thickness Mapping of the Central South Atlantic and the Geodynamic Development of the Rio Grande Rise and Walvis Ridge

Michelle Cunha Graça*[1,2], Nick Kusznir [3], Natasha Santos Gomes Stanton[1]

[1] Faculty of Oceanography, Rio de Janeiro State University, Rio de Janeiro, Brazil

[2] Geological Survey of Brazil – CPRM, 404, Pasteur Avenue, Urca, Rio de Janeiro, Brazil

[3] Department of Earth & Ocean Sciences, University of Liverpool, Liverpool L69 3BX, UK

*corresponding author: e-mail address: michelle.graca@cprm.gov.br

Abstract

The origin of the Rio Grande Rise and Walvis Ridge within the central South Atlantic and its implications for the separation of South America and Africa during the Cretaceous are controversial. The recent report of the discovery from submersible sampling of continental material of Proterozoic age on the Rio Grande Rise suggests that the existing explanation involving ocean ridge – mantle plume interaction or simply excess 'on-ridge' magmatism for the formation of the Rio Grande Rise and Walvis Ridge needs to be re-examined. We use gravity anomaly inversion to map crustal thickness for the central South Atlantic area encompassing the Rio Grande Rise, Walvis Ridge and adjacent South American and African rifted continental margins. We show that the Rio Grande Rise consists of three distinct bodies of anomalously thick crust (Western, Central and Eastern) separated by normal thickness oceanic crust. The Central Rio Grande Rise forms a large elliptical body with maximum crustal thickness of 25 km. The Walvis Ridge also has a maximum crustal thickness of 25 km but has a narrower and more linear geometry. We use plate reconstructions to restore maps of crustal thickness and magnetic anomaly to Early Cretaceous times to examine the development of the Rio Grande Rise and Walvis Ridge. These restorations together with ages

of magmatic addition suggest that the Central Rio Grande Rise and Walvis Ridge formed a single body between 90 and 80 Ma located on the ocean ridge plate boundary similar to Iceland today. On the basis of crustal thickness mapping, the plate restorations and the magmatic ages, we propose that the Rio Grande Rise was fragmented into its 3 parts and separated from Walvis Ridge by at least 4 ocean ridge jumps during the opening of the South Atlantic Ocean between approximately 90 and 50 Ma. Plate reconstructions of crustal thickness showing rotated structural lineaments imply that the separation of Eastern Rio Grande Rise and Walvis Ridge was highly complex involving simultaneous crustal extension and magmatic addition. We propose that the continental material reported on the Rio Grande Rise, if not drop-stones, was isolated from the main continental land-mass and transported into the ocean by these ridge jumps during the Cretaceous formation of the South Atlantic.

Keywords: Rio Grande Rise, Walvis Ridge, South Atlantic, Gravity anomaly inversion, Crustal thickness, Plate Reconstruction.

1. Introduction

The ocean basin of the central South Atlantic (Figure 1) is dominated by the Rio Grande Rise (RGR) and Walvis Ridge (WR). Both are spatially extensive regions of anomalously shallow bathymetry within an otherwise normal oceanic domain and are associated with Late Cretaceous and Cenozoic magmatism. The commonly held view is that both the RGR and WR were formed by the interaction of the Tristan da Cunha mantle plume with sea-floor spreading during the formation of the S. Atlantic (Wilson, 1963, 1965; Dietz and Holden, 1970; Morgan, 1971). The Early Cretaceous formation of the Paraná-Etendeka Magmatic provinces, the subsequent magma rich breakup of western Gondwana and initiation of sea-

floor spreading in the southern South Atlantic are also attributed to the Tristan da Cunha mantle plume, as are the Late Cretaceous to Cenozoic Tristan-Gough Guyot chains.

The expectation therefore is that the RGR and WR are oceanic crust greatly thickened by ocean ridge - mantle plume interaction or anomalous excess ocean ridge magmatism, similar to that believed to be responsible for the formation of the thick crust under Iceland today. However, recent geological sampling of the RGR indicates the presence of some continental material of Proterozoic age in the RGR. Reported submersible sampling found granites, granulites, gneisses, and pegmatites with ages between 500 and 2200 Ma (Fioravanti, 2014). If those continental rocks are not drop-stones, the discovery of continental material within the RGR suggests that the ocean ridge - mantle plume interaction hypothesis for RGR and WR formation needs to be reconsidered. Continental material has been found in other oceans significant distances from the nearest continental land-mass. Examples include the discovery of Pre-Cambrian zircons in Mauritius in the Indian Ocean (Torsvik et al., 2013) and geochemical evidence for continental material under SE Iceland (Torsvik et al., 2015). In both of these cases plate tectonic re-organisations and ridge jumps resulted in continental crust or subcontinental lithospheric mantle (SCLM) becoming isolated within the oceanic domain. Such a mechanism has not been proposed previously for the formation of the RGR and WR.

The RGR is located in oceanic lithosphere offshore of the Santos and Pelotas segments of the Brazilian rifted margin and is separated from the São Paulo Plateau and the Florianópolis Ridge by oceanic crust (Leyden et al., 1971). In this context, the presence of continental rocks with affinities with the adjacent continental lithosphere of Africa and South America raises questions about the nature, origin and kinematics of South Atlantic Ocean formation since the breakup of Western Gondwana.

The aim of this paper is to present the results of new detailed crustal thickness mapping using gravity inversion of the central South Atlantic area encompassing the RGR, WR and adjacent SouthAmerican and African rifted continental margins, and to use plate reconstructions to restore these crustal thickness maps to Early Cretaceous times in order to examine the development of the RGR and WR. The observed ages of magmatic additions and restored magnetic anomalies are also incorporated into our analysis. By doing so we aim to provide new observations and constraints on the formation mechanisms of the RGR and WR, and the development of the central South Atlantic.

2. **The Rio Grande Rise (RGR) and Walvis Ridge (WR)**

The Rio Grande Rise (RGR), along with its conjugate Walvis Ridge (WR), forms the two most prominent bathymetric features in the South Atlantic ocean basin (O'Connor and Duncan, 1990). The RGR extends between latitudes 28º and 34ºS and longitudes 28º and 40ºW. It is delimited to the north and south by the Rio Grande and 35.3 º S oceanic fractures zones and consists of seamounts, guyots and escarpments (Alves, 1981). Gamboa and Rabinowitz (1984) using geomorphology identified two distinct units: the Western and Eastern RGR. In this paper, we name these the Central (CRGR) and Eastern RGR (ERGR) units so we can also distinguish an additional distinct unit we call the Western RGR (WRGR) (Figure 2). In this paper the WRGR is considered as a RGR unit due to its similar crustal thickness, magnetic anomalies and proximity to the CRGR and ERGR The Western, Central and Eastern RGR are separated by oceanic abyssal plains with few seamounts. The Central RGR presents an elliptical bathymetric anomaly with extensive regions with bathymetry less than 1000 m (700 m at the shallowest point) compared with the regional oceanic bathymetry of greater than 4000 m. In comparison to the Central RGR, the Eastern RGR is much less well known. The Eastern RGR is composed of two main segments with average bathymetries of

2000 m. The Western RGR shows a much less pronounced bathymetric anomaly with shallowest values of approximately 3000 m.

Gamboa and Rabinowitz (1984) suggests that the RGR was first formed at the oceanic spreading center near to sea level in the Santonian-Coniacian and then thermally subsided accompanied by pelagic sedimentation. Afterwards, in the Middle Eocene, an alkaline volcanic episode uplifted the Central RGR creating numerous oceanic islands resulting in erosion and a sedimentation phase characterized by turbidite currents and landslides due to the extension of the underlying crust (Barker, 1983; Gamboa and Rabinowitz, 1984). Flexural isostasy analysis by Ussami et al. (2013) supports the interpretation that the RGR was constructed during these two main magmatic events. Subsequently, the RGR province returned to oceanic thermal subsidence and sedimentation (Detrick et al., 1977).

The Central RGR has a major rift-like structures aligned in a NW-SE direction which is associated with the Cruzeiro do Sul Lineament (Mohriak et al., 2010) and is partially filled with sediments. The Cruzeiro do Sul Lineament extends from the Cabo Frio High south-eastwards into the RGR and involves both continental and oceanic lithosphere. Walvis Ridge (WR) apparently does not show a zone of similar deformation (Mohriak et al., 2010). The Cabo Frio High, which divides the two largest oil producing provinces in Brazil, the Campos and Santos basins, appears to be the north-western continuation of the Cruzeiro do Sul Lineament (Souza et al., 1993). Seamounts and guyots are located along this rift-structure in the Central and Eastern RGR, suggesting that this volcanism was originated in the Middle Eocene (Barker, 1983) as a result of within-plate extensional stresses that caused mantle decompression and melting.

The WR is located in the eastern South Atlantic on the opposite side of the mid-Atlantic ridge in an approximately conjugate position to the RGR (Figure 1). It forms part of the

Tristan-Gough age-progressive magmatic track which connects the Etendeka Magmatic Province in the African continent with the Tristan da Cunha and Gough island groups in the ocean part of the African plate. In the north-east it comprises the aseismic Walvis Ridge itself, and the contiguous Guyot Province which extends in the south-west direction and which bifurcates in the south-west forming two spatially separate subtracks (the Tristan and Gough tracks) (Rohde et al., 2013). Fromm et al. (2017) modelled the P-wave velocity structure of northeastern segment of WR and proposed that it consists of thickened oceanic crust composed of basaltic layers, pillow basalts and sheeted dikes in the upper crust and gabbroic rocks in the lower crust.

The first explanations for the origin of these conjugate RGR and WR features were proposed by Wilson (1963, 1965), Dietz and Holden (1970) and Morgan (1971) who suggested that they were formed during the opening of the South Atlantic as the South American and African plates moved away from a stationary mantle “hot spot” located at the seafloor spreading axis. Kumar and Gambôa (1979) also suggested a RGR-WR common origin as resulting from an excess volcanism between 100 and 80 Ma in a segment of the southern mid-Atlantic ridge delimited by fracture zones. The flexural isostatic analysis of Ussami et al. (2013) is consistent with the results of South Atlantic palaeo-geographical reconstruction to anomaly C34 (at 84 Ma) which puts RGR and WR together on the ocean ridge. Following the generation of the Paraná-Etendeka Magmatic Province (PMP) during the Early Cretaceous, it has been proposed that the Tristan da Cunha-Gough mantle plume generated the RGR and WR at the ocean ridge spreading axis (Wilson, 1963; Morgan, 1971; O’Connor and Duncan, 1990). However RGR-WR morphologies differ from the expected "V" shaped symmetry about the sea-floor spreading axis mid-ocean ridge because at around 75 Ma multiple ocean ridge jumps occured in an eastward direction. This resulted in the isolation of the RGR from the spreading axis while the WR continued its formation by

intraplate volcanism generating the Guyot Province. Afterwards, during the transition of the WR to the Guyot Province, westward ocean ridge jumps also occurred (Rohde et al., 2013).

Ussami et al. (2013) found that RGR-WR basalts have isotope signatures with an EMI (Enriched Mantle I) component which are very different from those of N-MORB (Normal Mid-Ocean Ridge Basalt) indicating melting of a distinct mantle source without a continental crust melting component and distinct from the present-day Tristan da Cunha alkaline rocks. It is nearly identical to the PMP (Paraná Magmatic Province) tholeiites (133-132 Ma) (Figure 1). Isotopic data for the Eocene age alkaline basalts are still unknown.

Explanations of the origin of the EMI (Enriched Mantle I) component include thermal erosion of the Subcontinental Lithosperic Mantle (SCLM) due to small-scale convection at the edge of a cratonic lithosphere (King, 2000; King and Anderson, 1998), melting of fragments of delaminated or detached SCLM before, during and after continental break-up including mantle metasomatism and edge-driven convection (Peate et al., 1999; Smith and Lewis, 1999; Foley, 2008) and thermal erosion at the base of a SCLM and mantle flow transport (Class and le Roex, 2006; Meyzen et al., 2007). Detachment and/or thermal erosion of an old SCLM is the most accepted model to explain the EMI geochemical and isotope signatures of the RGR-WR (Hawkesworth et al., 1986; Peate et al., 1999; Gibson et al., 2005; Class and le Roex, 2006; Meyzen et al., 2007). This led Ussami et al. (2013) to suggest that RGR-WR magmatism results from melting of a heterogeneous lithospheric mantle which was fragmented and left behind during western Gondwana break-up. To maintain the deep mantle plume theory to explain South Atlantic magmatism with a EMI signature, it is necessary that the a mantle plume evolved in space and time (Ussami et al., 2013). Hoernle et al. (2015) consider a mantle plume to be the cause of the RGR-WR and present a spatial-temporal geochemical zonation for the Tristan-Gough age-progressive magmatic track.

Others studies examine the South Atlantic magmatic track, mainly for the African plate and WR, and suggest an origin at the core-mantle boundary (COB) deriving from the edge of the Africa Low Shear Wave Velocity Province (Burke et al., 2008; Torsvik et al., 2010; O'Connor et al., 2012; Steinberger and Torsvik, 2012). Some recent $^{40}Ar/^{39}Ar$ results explain the spatial and temporal distribution of the magmatism in the southeast Atlantic Ocean as being controlled by the interplay between deep-sourced mantle plumes and the motion and structure of the African plate. This requires a stable (or coherently moving) deep mantle source(s) to explain the parallel age-progressive magmatic trails (O'Connor et al., 2012; O'Connor and Jokat, 2015).

(Rohde et al., 2013) also dated RGR-WR basalts, tephrites, trachytes, and phonotephrites using $^{40}Ar/^{39}Ar$ method. Their research indicates an overall age progression volcanism along the Tristan-Gough track. According to Rohde et al. (2013), the age progression together with the decrease in the amount of volcanism along the Tristan-Gough track, suggests a genesis above a deep mantle plume, which began with the formation of the Paraná-Etendeka Magmatic Provinces. The plume then transitioned into a broad conduit centered on the ridge axis, forming the RGR-WR, and then became unstable and bifurcated around 60-70 Ma ago turned into pulsing "bubbles" between 35-45 Ma to form the Guyot Province (Rohde et al., 2013).

Galvão and Castro (2017) used magnetic anomalies from EMAG2 data (Maus et al., 2009), gravity data and plate reconstructions to interpret fracture zones in the Central and Eastern RGR and proposed that slivers of continental blocks rose during magma emplacement.

The WR emplacement has also been explained by the existence of a major fracture zone in the South Atlantic named Rio Grande Fracture Zone (RGFZ) (Figures 1 and 2). Some

authors assign the origin of the WR to the evolution of this fracture zone with an extensional component (a failed rift arm of a triple junction) producing volcanism (Le Pichon and Fox, 1971; Fairhead and Wilson, 2005; Elliott et al., 2009) or to a combination of hotspot and fracture zone mechanism (Haxel, 2005). In contrast Fromm et al. (2017) modelled the P-wave velocity structure of the eastern segment of the WR and concluded that the RGFZ and WR evolved independently from each other.

3. Data and Methodology

We use public domain free-air gravity anomaly, bathymetry and sediment thickness data to determine crustal thickness for the RGR, WR and adjacent South Atlantic Ocean region. The bathymetric data (Figures 1 and 2) used was taken from the ETOPO1 compilation provided by the National Geophysical Data Center (NGDC) and described in Amante and Eakins (2009). The free-air gravity anomaly data (Figure 3a) were derived from satellite radar altimetry (Sandwell and Smith, 2009). Sediment thicknesses were taken from the NGDC global marine compilation (Divins, 2003). We also compare the free-air gravity anomaly data and crustal thickness distribution with regional magnetic anomaly from EMAG2 (version 3). EMAG2 v3 (Figure 3b) is a compilation of marine, terrestrial, aerial and satellite magnetic measurements with a lateral resolution of 2 arc-minutes, an anomaly altitude at sea level for oceanic regions and 4 km for continental regions, a maximum degree or order of 300 and minimum wavelength within our study area of 15 km (Meyer et al., 2017).

Regional crustal basement thickness has been determined using 3D gravity inversion which is carried out in the spectral domain and incorporates a lithosphere thermal gravity anomaly correction. The gravity inversion technique used is described in detail in Chappell and Kusznir (2008) and Alvey et al. (2008). It is important to include a correction for the lithosphere thermal gravity anomaly because of the elevated geotherm of oceanic and

continental margin lithosphere; failure to do so leads to a significant over-estimate of Moho depth and crustal basement thickness.

The lithosphere thermal gravity anomaly correction requires information on the lithosphere cooling time and also the magnitude of the initial lithosphere thermal pertubation. For oceanic regions, the ocean isochrons of (Müller et al., 2008) were used to give cooling ages and a lithosphere thinning factor (1-1/β) of 1 to derive the initial thermal perturbation (β is the lithosphere stretching factor defined by McKenzie (1978) and is ∞ for oceanic lithosphere). For the continental margin lithosphere, the breakup age is used for the lithosphere cooling time and the lithosphere thinning factor for the initial thermal perturbation is derived from the gravity inversion itself (see Chappell and Kusznir (2008) for further explanation).

The sediment density used in the gravity inversion assumes a compaction controlled dependence on depth corresponding to shaly-sand lithology (Sclater and Christie, 1980). We use a crustal basement density of 2850 kg/m^3 and a mantle density of 3300 kg/m^3.

Crustal thickness derived from gravity inversion using public domain NGDC sediment thickness is shown in Figure 4a. The input data used in the gravity inversion consists of bathymetry, free-air gravity anomaly and sediment thickness. Of these, the least accurate is sediment thickness. As a consequence we compare crustal thickness predicted by gravity inversion for a profile for which we have more accurate sediment thickness derived from seismic reflection data across the RGR with that using the NGDC global sediment thickness compilation. The location of the profile is shown in Figure 4a. The seismic reflection data along this profile crossing the RGR was acquired by the Institute for Geophysics of the University of Texas at Austin (Barker, 1983; Gamboa and Rabinowitz, 1984) and a regional Leplac seismic profile (L511) reported in Mohriak et al. (2010). Figure 4b&c show Moho

depth and crustal basement thickness derived from gravity inversion along this profile using sediment thickness from the seismic reflection data and the global NGDC compilation. Comparison shows that the gravity inversion using the global NGDC sediment thickness compilation gives a similar Moho depth and crustal thickness to that derived using seismic reflection sediment thicknesses. As a consequence we believe that the gravity inversion mapping of crustal thickness using the NGDC public domain sediment thickness is meaningful and useful.

In Figure 4b,c&d we also compare Moho depth derived from gravity inversion with independent seismic reflection measurements from Constantino et al. (2017). The comparison suggests that the gravity inversion method provides a reliable estimate of Moho depth and crustal thickness which allows the regional S. Atlantic mapping of these parameters. The cross-plot shown in Figure 4d has been used to calibrate the reference Moho depth used in the gravity inversion and gives a value for this parameter of 35 km.

If a heterogeneous lithospheric mantle which was fragmented and left behind during western Gondwana break-up (Ussami et al. 2013) was incorporated in the gravity inversion, it would modify the lithosphere temperature structure used to calculate the lithophere thermal gravity anomaly correction. If this resulted in a slightly cooler lithoshere under the RGR then this would reduce the thermal correction and give a slightly thicker crust.

4. RGR, WR and South Atlantic crustal thickness distribution

Figure 5 shows the crustal thickness map of South Atlantic Ocean, including the RGR and WR, derived from gravity inversion. It shows that while the South Atlantic generally has oceanic crust of normal thickness (7 +/- 1 km), the Central and Eastern RGR and the WR show much thicker crust with maximum crustal thickness of approximately 25 km (see Figure

4b&c also). Other features with significant thick crust (> 15 km) are the Western RGR, Florianópolis Ridge, São Paulo Plateau and Torres High. The Torres High, a feature that runs from the Ponta Grossa Arch (Figure 2) on the continental margin into the ocean, interconnects with the Western RGR. The African continental margin has a different appearance compared with the Brazilian continental margin. There is a direct connection between WR and the continent through Namibia Ridge, and it does not have defined features with thick crust like the São Paulo Plateau and Florianópolis Ridge.

Magmatic ages (Renne et al., 1996; O'Connor et al., 2012; Rohde et al., 2013; Geraldes et al., 2013; Hoernle et al., 2015; O'Connor and Jokat, 2015) for the RGR, WR, Guyot Province, Africa and South America are superimposed on the crustal thickness map shown in Figure 5. The RGR has magmatic ages between 80 – 87 Ma and 46 Ma, while WR has ages from 114 Ma in its northern segment decreasing to 1 Ma at its southern end. While RGR and WR magmatic ages may correlate for the northern segment of WR, in the southwest of WR its ages are much younger than the RGR magmatic ages. Figure 5 shows that WR ages decrease southwestwards from the African continent towards the present mid-ocean ridge.

Three regional crustal cross-sections crossing the RGR have been constructed using bathymetry, sediment thickness and Moho depth from gravity anomaly inversion and compared with magnetic anomaly data. Profile AB (Figure 6b), which runs west to east from the Pelotas margin oceanwards across the RGR, shows the three main units of the RGR, the Western, Central and Eastern RGR, which are characterized by deep Moho, thick crust and high amplitude magnetic anomalies. They are separated by oceanic crust of normal, or near normal, thickness. Along profile AB both Western and Eastern RGR have similar Moho depths, reaching 17 km. The deepest Moho is located in the Central RGR (> 25 km) and is correlated with a very large magnetic anomaly (C34) reaching 450 nT. The rift valley

associated with the Cruzeiro do Sul Lineament can be seen on profile AB and is located above where the the Central RGR has maximum crustal thickness.

Cross-section CD shown in Figure 6c runs from the Santos Basin oceanwards in a SE direction and also crosses the Central RGR. The maximum Moho depth on this profile also reaches 25 km on the Central RGR. The cross-section shows that Central RGR is separated from the Florianópolis Ridge (and the São Paulo Plateau) by much thinner crust of approximately 10 km thickness in the region of the Rio Grande Fracture Zone. The Florianópolis Ridge and São Paulo Plateau have Moho depth of approximately 20 km and 15 km respectively. The crustal thickness map (Figure 6a) also shows that the entire Central RGR has substantially thicker crust than the São Paulo Plateau and Florianópolis Ridge and presents a significant crustal thickness anomaly. The anomalously thick crust under the Central RGR predicted by gravity inversion is isostatically consistent with the bathymetry of this region which is locally less than 1 km. In contrast the thinner crust of the São Paulo Plateau has a greater bathymetry of over 2 km despite its greater sediment thickness. The thicker crust of the Central RGR and Florianópolis Ridge correlate with high amplitude magnetic anomalies.

Cross-section EF (Figure 6d) runs N-S and cuts the Central RGR where Moho depth increases abruptly reaching more than 25 km depth. To both the north and south of the Central RGR, crustal thickness decreases to as low as 5 km corresponding to normal, or slightly thinner than normal, oceanic crust. The magnetic anomaly along the EF profile is not shown because of its N-S orientation.

A direct correlation between thicker crust and large amplitude magnetic anomalies is observed for all components of the RGR; 200 nT for Western RGR, 450 nT for Central RGR and more than 200 nT for Eastern RGR. This suggests that igneous rocks from oceanic crust

are present in the RGR and possibly contribute to the anomalously large crustal thicknesses. Shallow bathymetry with igneous rocks from oceanic crust may also generate the higher amplitude magnetic anomalies.

No important magnetic anomaly indicating a large block of non-magnetic continental crust seems to be present. A magnetic anomaly signature from continental upper crust rocks (sedimentary, acid igneous and metamorphic rocks) with less magnitite content and remanent magnetization compared with basic igneous and volcanic rocks has not been identified. If it had been present this would have generated a large reversed polarity induced magnetic anomaly.

However the presence of excess magmatism within the RGR does not necessarily exclude interaction between continental and oceanic crust or lithospheric mantle within the RGR, as evidenced by the rock samples of continental origin collected on the RGR.

5. Magnetic Anomalies, Crustal Thickness and Plate Reconstructions between 90 and 70 Ma

Maps of crustal basement thickness from gravity inversion and magnetic anomalies (Figures 3b and 5) have been restored to ages of 90, 80 and 70 Ma using the Gplates 1.5 plate reconstruction software with rotation poles, plate polygons and ocean isochrones from Seton et al. (2012).

South Atlantic magnetic anomalies are characterized by two main zones with different anomaly patterns. The Cretaceous Normal Superchron (CNS), which runs oceanwards from the Brazilian and African margin until anomaly C34 (83 Ma) and represents a long period of stable polarity of the geomagnetic field with small amplitude anomalies. Further oceanwards the younger magnetic anomaly pattern from C34 to the present turns into a typical oceanic

striped pattern formed by normal oceanic sea-floor spreading and geomagmetic field reversals.

For the South Atlantic ocean floor reconstructions, the spreading history along the entire length of the South Atlantic from Anomaly 34 (83.5 Ma) onwards is relatively uncomplicated. Most studies are in agreement and propose largely symmetrical sea-floor spreading occurred after Anomaly 34 to the present day (Rabinowitz and Labrecque, 1977; Nürnberg and Müller, 1991; Cande and Kent, 1992; Moulin et al., 2010; Seton et al., 2012). However it is difficult to determine reconstructions before the Anomaly 34 during the Cretaceous Normal Superchron (CNS) (Pindell et al., 1988; Nürnberg and Müller, 1991; Müller et al., 1998;).

In Figure 7, the 90 Ma reconstruction only shows magnetic anomalies of the CNS (Cretaceous Normal Superchron). According to the magmatic ages presented in Figure 5, the magmatic components of the Central and Eastern RGR had not been formed by this time. By 80 Ma, the large negative magnetic anomaly corresponding to the C34 isochron are present and pass through the Central RGR and WR which appear to form a single body at this time as shown by the restored crustal thickness map. This C34 magnetic anomaly marks the divergent plate boundary at 83 Ma and we therefore interpret this to indicate that the combined Central RGR and WR were located at the divergent plate boundary at this time. The Central RGR has basalt ages between 80 and 87 Ma coincident with this period. Therefore between 90 and 80 Ma, the restored magnetic anomaly and crustal thickness maps bring together RGR and WR as a single body with active magmatism located above the sea-floor spreading axis. This is a similar configuration to Iceland today (Torsvik et al., 2015).

Although the Tristan-Gough age-progressive magmatic track appears in the 80 Ma reconstruction shown in Figure 7, its magmatic ages indicate its emergence starting about at 70 Ma, as shown in the plate reconstruction at this time. During the same time interval (80 -

70 Ma), the Eastern RGR emerges and has started to separate from WR at 70 Ma. By 70 Ma the Central RGR was distinct and separated from the WR.

Figure 8a shows the crustal basement thickness map from gravity inversion restored to 83 Ma when Central RGR and WR were a single combined feature above an active ocean ridge. Figure 8b shows a crustal cross-section along profile RW running E-W across the Western RGR, Vema Channel, Central RGR and WR respectively. Note that at 83 Ma the restoration suggest that the Eastern RGR had not yet been formed. Maximum Moho depths on the Central RGR and WR reach 25 km. The region of thick crust under the Central RGR is wider that under the WR. Crustal thickness exceeds 20 km for the Central RGR for a profile distance of more than 500 km while for the WR the corresponding extent is 150 km.

It is notable that the shape of the regions of thick crust under the Central RGR and the WR are different; thick crust under the Central RGR has an elliptical shape while that for the WR is more linear.

WR shows continuity of crustal thickness from continent to ocean (Namibia Ridge-Walvis Ridge-Tristan Gough track). In contrast, RGR is fragmented into three units and the Central and Eastern RGR do not show connection in any obvious way with the continent. The Western RGR may have been connected to the Torres High, Florianópolis Ridge and São Paulo Plateau but is now separated. This could be indicative of multiple plate boundaries re-organizations and ocean-ridge jumps during the early formation of the S. Atlantic.

Both the Central RGR and the WR show large magnetic anomalies (Figure 8b). Their maximum crustal thickness of 25 km, their high amplitude magnetic anomalies and the plate restorations all suggest a direct relationship between Central RGR and WR.

Profile RW (Figure 8b) also crosses the Western RGR where a maximum crustal thickness of 12 km is reached. Thin crust of normal oceanic thickness (or less) is seen to the

west of the Western RGR and to the east between the Western and Central WGR (in the Vema Channel).

6. Crustal Structure and Plate Reconstructions from 70 Ma to present day

Figure 9 shows plate restorations of crustal thickness from gravity inversion from 70 to 40 Ma at 10 Myr intervals. By 50 Ma the Eastern RGR and WR had separated; this may have occurred by 60 Ma. The separation coincides with the transition from mantle plume - plate boundary interaction and/or enhanced magmatism above the ocean spreading center to off-ridge intraplate magmatism. The change of the Tristan da Cunha mantle plume to off-ridge magmatism generates the Tristan-Gouch volcanic track in pre-existing oceanic lithosphere which continues to the present day. This change from on-ridge to off-ridge mantle plume magmatism has already beend described by O'Connor and Duncan (1990). Alternatively, the enhanced magmatism could have ceased on the ocean ridge and started off-ridge at approximately the same time. As shown in Figure 9, the separation process between Eastern RGR and WR (specifically the Tristan-Gough age-progressive magmatic track) lasted for about 20 Myr from 70 to 50 Ma.

Figure 10a shows crustal thickness from gravity inversion restored to 54 Ma. This restoration shows that the fracture zones connecting Eastern RGR and WR have a curved morphology showing rotations in the evolution of the separation of Eastern RGR from WR. These rotated fracture zones do not exist to the north or south of the Eastern RGR and stop at its north and south terminations, indicating that this region underwent differential deformation and extension. What causes this rotational deformation may be explained by variations in spreading rates in the mid-ocean ridge at that time but also may be indicative of more than one active spreading center at this period. This period of complex extension and deformation

probably not only affected the Eastern RGR but also WR and may have some influence in Guyot Province bifurcation.

The cross-sections (Figure 10b) along the axes of the Eastern RGR and WR show thick crust reaching almost 20 km thickness. Both cross-sections show thicker crust in the north than in the south. They also show high amplitude magnetic anomalies. In contrast the maps show that the thick crust of the Eastern RGR and WR are separated by oceanic crust of normal thickness.

The magnetic anomalies in the RGR (Figure 3b) show three distinct domains, representing the 3 different components of the RGR (Figure 2). Near the coast, a series of NE-SW short magnetic anomalies are observed, extending from the margin to the Central RGR, gradually shifting orientation to N-S (in the Western RGR) and to NNW-SSE (in the Central RGR) indicating rotation. This variation in magnetic anomaly orientation from NE-SW, parallel to the margin, to N-S in the Western RGR, to NW-SE in the Central RGR suggests rotation. In the Central RGR, the NW direction is distinct from the general anomaly orientation and probably reflects one or more changes in the oceanic spreading rates. In addition, oceanic spreading rates (Müller et al., 2008) indicate higher sea-floor spreading velocities in the south-east portion of the Central RGR than in the north, suggesting an internal deformationof this region. The Eastern RGR has a distinct magnetic anomaly set, with a large positive anomaly without a clear orientation of magnetic lineaments.

7. The role of ridge jumps in Western Gondwana separation

Together with intense magmatism, intra-ocean ridge jumps seem to be an important process in the South Atlantic evolution, especially in the formation of the RGR and WR. The present day asymmetry of the South Atlantic spreading-axis has been attributed to a

succession of easterly and southeasterly ocean ridge migrations prior to C34 (O'Connor and Duncan, 1990).

The first recorded eastward migration occurred to the north of the Torres High and WR in early Albian-late Aptian time (Leyden et al., 1971; Ponte and Asmus, 1976; Cande and Rabinowitz, 1978, 1979; Kumar and Gambôa, 1979; Rabinowitz and LaBrecque, 1979). A major sea-floor spreading ridge jump has also been proposed for the formation of the São Paulo Plateau on the SE Brazilian margin by transferring onto the South American plate a thickened piece of oceanic crust which was originally part of the African plate north of the Namibia Ridge (Pérez-Diaz and Eagles, 2014; Fromm et al., 2015). Kumar and Gambôa (1979) identified a N-S structure, between the Western and Central RGR in the Vema channel, as possibly being an extinct spreading center. Constantino et al. (2017) proposed that this feature extends northwards from 34ºS into the Florianópolis Ridge and called this feature as the Vema Aborted Ridge (VAR).Figure 11 shows crustal thickness from gravity inversion restored to 50 Ma, on which we identify past sea-floor spreading centres south of the Rio Grande Fracture Zone between the Torres High, the Western, Central and Eastern components of the RGR and the WR. The arrows in Figure 11 show distinct regions of oceanic crust generated as a consequence of the ridge jumps. They strike at different angles because of the extinct spreading centers original direction, the different velocities of the spreading rates and the rotation of the macroplates (the clockwise rotation of South American plate relative to Africa) and microplates, as indicated by curved fracture zones between the CRGR and ERGR.

In the region of Figure 4, we suggest that the sea-floor spreading was initially between the Torres High and the Western RGR (location 1 on Figure 11) before jumping to location 2 in the Vema Channel. The jump from ridge position 1 to position 2 in the Vema Channel would have separated the Western RGR from whatever lay to the east of it. This may have been the Namibian margin; at the time of this ridge jump the Central and Eastern RGR and

WR may not have existed as we know them at present. Sea floor spreading resulting from this ridge jump into the Vema Channel shows a strong asymmetry of accreted oceanic crust in the spreading corridor occupied by Vema Channel. Pérez-Diaz and Eagles (2014) propose an eastward migration of sea-floor spreading of 400 km for the jump from ridge position 1 to 2 which is consistent with what we see in Figures 4 and 11. The different shapes of the Central and Eastern RGR and WR may also have been the result of ridge jumps as suggested by Gamboa and Rabinowitz (1984). At approximately 80 Ma the Central RGR rifted and separated from the WR (which then included the Eastern RGR). This required an eastward migration or jump of sea-floor spreading to ridge position 3. By 70 Ma this was followed by rifting and separation of the Eastern RGR from the WR and required an additional eastward jump of rifting and sea-floor spreading to ridge position 4 from which it evolved to the present day. It is noteworthy that the African side of the S. Atlantic is much simpler than the S. American side, consistent with dominantly eastward migrations and jumps of the sea-floor spreading axes.

We propose that these successive ocean ridge jumps and plate boundary re-organizations were the main mechanism that formed the 3 separate components of the RGR and the WR. In addition we suggest that these jumps in rifting and sea-floor spreading isolated fragments of continental crust or lithospheric mantle from their original continental land-mass locations and transported them large distances into the oceanic domain. This may support the reports of continental material recovered by submersibles on the Central RGR. The dominantly eastward migration and jumps of rifting and sea-floor spreading may imply that continental fragments within the central S. Atlantic are likely to have an African affinity even though they are now located on the S. American plate.

Some important questions remain unanswered. When and where exactly did those ridges jumps take place? Were they simultaneously active? What is the generic relationship between ridge jumps, magmatism and continental crust in the oceanic realm?

8.Summary

We observe anomalously thick crustal thickness predicted by gravity inversion for the Western, Central and Eastern RGR and the WR. Both the Central RGR and the WR have maximum crustal thicknesses of 25 km which are substantially greater than that of surrounding S. Atlantic oceanic crust which has normal oceanic crustal thickness. The RGR also has thicker crust compared with the São Paulo Plateau and Florianópolis Ridge on the adjacent Brazilian continental margin.

There is a direct correlation between anomalously thick crust and high positive amplitude magnetic anomalies, suggesting that igneous rocks are present within the RGR and WR, which is already proven by DSDP drilling and coring. The anomalously large crustal thicknesses under the RGR and WR are most likely the result of magmatic addition but they may contain some continental material as shown by submersible sampling on the RGR. Gravity inversion alone cannot distinguish between continental and oceanic crust, however no significant magnetic anomaly indicating a large block of non-magnetic continental crust seems to be present.

The plate reconstruction of the C34 magnetic anomaly at 80 Ma shows the location of the South Atlantic divergent plate boundaries and ocean ridge. Restoration of crustal thickness from gravity inversion to 80 Ma shows that the C34 magnetic anomaly intersects the RGR and WR which at that time forming a single body. The reported magmatic ages of

the RGR and WR are consistent with this conclusion. The similar crustal thickness, high amplitude magnetic anomalies and the plate restorations suggest a direct relationship between RGR and WR and, therefore, a likely common origin. While at 80 Ma the RGR and WR form a single body located on the divergent plate boundary similar to Iceland today, by 70 Ma they are separated.

The Western, Central and Eastern RGR and the WR were separated by a series of eastward migrations and jumps of rifting and sea-floor spreading. These rift jumps may have isolated fragments of continental crust or lithospheric mantle from their original continental locations and transported them large distances into the oceanic domain of the S. Atlantic.

Existing models of the formation of the RGR and WR during S. Atlantic Ocean formation invoke ocean ridge – mantle plume interaction or anomalous 'on-ridge' magmatism to generate large magmatic thicknesses during sea-floor spreading. This interaction alone cannot however explain the reported discovery of Proterozoic material of continental affinity on the Central RGR. If those are not drop-stones, we suggest that the isolation and transport of fragments of continental crust or lithospheric mantle into the ocean domain by a series of eastward ridge jumps during the formation of the Central South Atlantic also plays an important role in the formation of the RGR and WR.

Acknowledgements

We would like to thank Prof. Renata Schmitt and Andres Gordon for the helpful comments and MM4 for providing useful discussions.

References

Alves, E.C., 1981. Geologia da margem continental sudeste/sul brasileira e das áreas continentais emersas e oceânicas adjacentes. Estruturas e tectonismo da margem Cont. Bras. e suas implicações nos Process. sedimentares e avaliação do potencial Recur. minerais. Série Proj. REMAC, PETROBRAS/DNPMCPRM/DHN/CNPq 9, 145–170.

Alvey, A., Gaina, C., Kusznir, N.J., Torsvik, T.H., 2008. Integrated crustal thickness mapping and plate reconstructions for the high Arctic. Earth Planet. Sci. Lett. 274, 310–321. https://doi.org/10.1016/j.epsl.2008.07.036

Amante, C., Eakins, B.W., 2009. ETOPO1 1 Arc-Minute Global Relief Model: Procedures, Data Sources and Analysis, NOAA Technical Memorandum NESDIS NGDC-24. https://doi.org/10.1594/PANGAEA.769615

Barker, P.F., 1983. Tectonic Evolution and Subsidence History of the Rio Grande Rise, in: Initial Reports of the Deep Sea Drilling Project, 72. U.S. Government Printing Office. https://doi.org/10.2973/dsdp.proc.72.151.1983

Burke, K., Steinberger, B., Torsvik, T.H., Smethurst, M.A., 2008. Plume Generation Zones at the margins of Large Low Shear Velocity Provinces on the core–mantle boundary. Earth Planet. Sci. Lett. 265, 49–60. https://doi.org/10.1016/j.epsl.2007.09.042

Cande, S.C., Kent, D. V., 1992. A new geomagnetic polarity time scale for the Late Cretaceous and Cenozoic. J. Geophys. Res. https://doi.org/10.1029/92JB01202

Cande, S.C., Rabinowitz, P.D., 1979. Magnetic Anomalies of the Continental Margin of Brazil 1: 4 000 000. American Association of Petroleum Geologists.

Cande, S.C., Rabinowitz, P.D., 1978. Mesozoic seafloor spreading bordering conjugate continental margins of Angola and Brazil, in: Offshore Technology Conference.

Chappell, A.R., Kusznir, N.J., 2008. Three-dimensional gravity inversion for Moho depth at rifted continental margins incorporating a lithosphere thermal gravity anomaly correction. Geophys. J. Int. 174, 1–13. https://doi.org/10.1111/j.1365-

246X.2008.03803.x

Class, C., le Roex, A.P., 2006. Continental material in the shallow oceanic mantle—How does it get there? Geology 34, 129. https://doi.org/10.1130/G21943.1

Constantino, R.R., Hackspacher, P.C., de Souza, I.A., Lima Costa, I.S., 2017. Basement structures over Rio Grande Rise from gravity inversion. J. South Am. Earth Sci. 75, 85–91. https://doi.org/10.1016/j.jsames.2017.02.005

Detrick, R.S., Sclater, J.G., Thiede, J., 1977. The subsidence of aseismic ridges. Earth Planet. Sci. Lett. https://doi.org/10.1016/0012-821X(77)90003-6

Dietz, R.S., Holden, J.C., 1970. Reconstruction of Pangaea: Breakup and dispersion of continents, Permian to Present. J. Geophys. Res. https://doi.org/10.1029/JB075i026p04939

Divins, D.L., 2003. Total Sediment Thickness of the World's Oceans and Marginal Seas, NOAA National Geophysical Data Center, Boulder, CO.

Elliott, G.M., Berndt, C., Parson, L.M., 2009. The SW African volcanic rifted margin and the initiation of the Walvis Ridge, South Atlantic. Mar. Geophys. Res. https://doi.org/10.1007/s11001-009-9077-x

Fairhead, J.D., Wilson, M., 2005. Plate tectonic processes in the South Atlantic Ocean: Do we need deep mantle plumes?, in: Special Paper 388: Plates, Plumes and Paradigms. Geological Society of America, pp. 537–553. https://doi.org/10.1130/0-8137-2388-4.537

Fioravanti, C., 2014. Ecos da separação - Grandes blocos de rochas com idades e origens diferentes se combinaram ao formar os dois lados do Atlantico Sul. Pesqui. Fapesp 224, 58–61.

Foley, S.F., 2008. Rejuvenation and erosion of the cratonic lithosphere. Nat. Geosci. 1, 503–510. https://doi.org/10.1038/ngeo261

Fromm, T., Jokat, W., Behrmann, J.H., 2017. Interaction between a hotspot and a fracture

zone: The crustal structure of Walvis Ridge at 6° E. Tectonophysics 716, 108–120. https://doi.org/10.1016/j.tecto.2017.03.001

Fromm, T., Planert, L., Jokat, W., Ryberg, T., Behrmann, J.H., Weber, M.H., Haberland, C., 2015. South Atlantic opening: A plume-induced breakup? Geology 43, 931–934. https://doi.org/10.1130/G36936.1

Galvão, I.L.G., de Castro, D.L., 2017. Contribution of global potential field data to the tectonic reconstruction of the Rio Grande Rise in the South Atlantic. Mar. Pet. Geol. https://doi.org/10.1016/j.marpetgeo.2017.06.048

Gamboa, L.A.P., Rabinowitz, P.D., 1984. The evolution of the Rio Grande Rise in the southwest Atlantic Ocean. Mar. Geol. https://doi.org/10.1016/0025-3227(84)90115-4

Geraldes, M.C., Motoki, A., Costa, A., Mota, C.E., Mohriak, W.E., 2013. Geochronology (Ar/Ar and K–Ar) of the South Atlantic post-break-up magmatism. Geol. Soc. London, Spec. Publ. 369, 41–74. https://doi.org/10.1144/SP369.21

Gibson, S.A., Thompson, R.N., Day, J.A., Humphris, S.E., Dickin, A.P., 2005. Melt-generation processes associated with the Tristan mantle plume: Constraints on the origin of EM-1. Earth Planet. Sci. Lett. 237, 744–767. https://doi.org/10.1016/j.epsl.2005.06.015

Hawkesworth, C.J., Mantovani, M.S.M., Taylor, P.N., Palacz, Z., 1986. Evidence from the Parana of south Brazil for a continental contribution to Dupal basalts. Nature 322, 356–359. https://doi.org/10.1038/322356a0

Haxel, J.H., 2005. Evidence of explosive seafloor volcanic activity from the Walvis Ridge, South Atlantic Ocean. Geophys. Res. Lett. 32, L13609. https://doi.org/10.1029/2005GL023205

Hoernle, K., Rohde, J., Hauff, F., Garbe-Schönberg, D., Homrighausen, S., Werner, R., Morgan, J.P., 2015. How and when plume zonation appeared during the 132 Myr

evolution of the Tristan Hotspot. Nat. Commun. 6, 7799. https://doi.org/10.1038/ncomms8799

King, S.D., 2000. African Hot Spot Volcanism: Small-Scale Convection in the Upper Mantle Beneath Cratons. Science (80-.). 290, 1137–1140. https://doi.org/10.1126/science.290.5494.1137

King, S.D., Anderson, D.L., 1998. Edge-driven convection. Earth Planet. Sci. Lett. 160, 289–296. https://doi.org/10.1016/S0012-821X(98)00089-2

KUMAR, N., GAMBÔA, L.A.P., 1979. Evolution of the São Paulo Plateau (southeastern Brazilian margin) and implications for the early history of the South Atlantic. Geol. Soc. Am. Bull. 90, 281. https://doi.org/10.1130/0016-7606(1979)90<281:EOTSPP>2.0.CO;2

Le Pichon, X., Fox, P.J., 1971. Marginal offsets, fracture zones, and the early opening of the North Atlantic. J. Geophys. Res. 76, 6294–6308. https://doi.org/10.1029/JB076i026p06294

Leyden, R., Ludwig, W.J., EWING, M., 1971. Structure of continental margin off Punta del Este, Uruguay, and Rio de Janeiro, Brazil. Am. Assoc. Pet. Geol. Bull. https://doi.org/10.1306/819A3E2A-16C5-11D7-8645000102C1865D

Maus, S., Barckhausen, U., Berkenbosch, H., Bournas, N., Brozena, J., Childers, V., Dostaler, F., Fairhead, J.D., Finn, C., Von Frese, R.R.B., Gaina, C., Golynsky, S., Kucks, R., Lühr, H., Milligan, P., Mogren, S., Müller, R.D., Olesen, O., Pilkington, M., Saltus, R., Schreckenberger, B., Thébault, E., Tontini, F.C., 2009. EMAG2: A 2-arc min resolution Earth Magnetic Anomaly Grid compiled from satellite, airborne, and marine magnetic measurements. Geochemistry, Geophys. Geosystems. https://doi.org/10.1029/2009GC002471

MCKENZIE, D., 1978. Some remarks on the development of sedimentary basins. Earth Planet. Sci. Lett. 40, 25–32. https://doi.org/10.1016/0012-821X(78)90071-7

Meyer, B., Chulliat, A., Saltus, R., 2017. Derivation and Error Analysis of the Earth Magnetic Anomaly Grid at 2 arc min Resolution Version 3 (EMAG2v3). Geochemistry, Geophys. Geosystems 18, 4522–4537. https://doi.org/10.1002/2017GC007280

Meyzen, C.M., Blichert-Toft, J., Ludden, J.N., Humler, E., Mével, C., Albarède, F., 2007. Isotopic portrayal of the Earth's upper mantle flow field. Nature 447, 1069–1074. https://doi.org/10.1038/nature05920

Mohriak, W.U., Nobrega, M., Odegard, M.E., Gomes, B.S., Dickson, W.G., 2010. Geological and geophysical interpretation of the Rio Grande Rise, south-eastern Brazilian margin: extensional tectonics and rifting of continental and oceanic crusts. Pet. Geosci. https://doi.org/10.1144/1354-079309-910

Morgan, W.J., 1971. Convection plumes in the lower mantle. Nature. https://doi.org/10.1038/230042a0

Moulin, M., Aslanian, D., Unternehr, P., 2010. A new starting point for the South and Equatorial Atlantic Ocean. Earth-Science Rev. https://doi.org/10.1016/j.earscirev.2009.08.001

Müller, R.D., Roest, W.R., Royer, J.Y., 1998. Asymmetric sea-floor spreading caused by ridge-plume interactions. Nature. https://doi.org/10.1038/24850

Müller, R.D., Sdrolias, M., Gaina, C., Roest, W.R., 2008. Age, spreading rates, and spreading asymmetry of the world's ocean crust. Geochemistry, Geophys. Geosystems. https://doi.org/10.1029/2007GC001743

Nürnberg, D., Müller, R.D., 1991. The tectonic evolution of the South Atlantic from Late Jurassic to present. Tectonophysics. https://doi.org/10.1016/0040-1951(91)90231-G

O'Connor, J.M., Duncan, R.A., 1990. Evolution of the Walvis Ridge-Rio Grande Rise Hot Spot System: Implications for African and South American Plate motions over plumes. J. Geophys. Res. https://doi.org/10.1029/JB095iB11p17475

O'Connor, J.M., Jokat, W., 2015. Tracking the Tristan-Gough mantle plume using discrete chains of intraplate volcanic centers buried in the Walvis Ridge. Geology 43, 715–718. https://doi.org/10.1130/G36767.1

O'Connor, J.M., Jokat, W., le Roex, A.P., Class, C., Wijbrans, J.R., Keßling, S., Kuiper, K.F., Nebel, O., 2012. Hotspot trails in the South Atlantic controlled by plume and plate tectonic processes. Nat. Geosci. 5, 735–738. https://doi.org/10.1038/ngeo1583

Peate, D.W., Hawkesworth, C.J., Mantovani, M.M.S., Rogers, N.W., Turner, S.P., 1999. Petrogenesis and Stratigraphy of the High-Ti/Y Urubici Magma Type in the Parana Flood Basalt Province and Implications for the Nature of 'Dupal'-Type Mantle in the South Atlantic Region. J. Petrol. 40, 451–473. https://doi.org/10.1093/petroj/40.3.451

Pérez-Díaz, L., Eagles, G., 2014. Constraining South Atlantic growth with seafloor spreading data. Tectonics 33, 1848–1873. https://doi.org/10.1002/2014TC003644

Pindell, J.L., Cande, S.C., Pitman, W.C., Rowley, D.B., Dewey, J.F., Labrecque, J., Haxby, W., 1988. A plate-kinematic framework for models of Caribbean evolution. Tectonophysics. https://doi.org/10.1016/0040-1951(88)90262-4

Ponte, F.C., Asmus, H.E., 1976. The Brazilian marginal basins: current state of knowledge. An. Acad. Bras. Cienc. 48, 215–329.

Rabinowitz, P.D., LaBrecque, J., 1979. The Mesozoic South Atlantic Ocean and evolution of its continental margins. J. Geophys. Res. 84, 5973. https://doi.org/10.1029/JB084iB11p05973

Rabinowitz, P.D., Labrecque, J.L., 1977. The isostatic gravity anomaly: key to the evolution of the ocean-continent boundary at passive continental margins. Earth Planet. Sci. Lett. https://doi.org/10.1016/0012-821X(77)90037-1

Renne, P.R., Glen, J.M., Milner, S.C., Duncan, A.R., 1996. Age of Etendeka flood volcanism and associated intrusions in southwestern Africa. Geology 24, 659.

https://doi.org/10.1130/0091-7613(1996)024<0659:AOEFVA>2.3.CO;2

Rohde, J.K., van den Bogaard, P., Hoernle, K., Hauff, F., Werner, R., 2013. Evidence for an age progression along the Tristan-Gough volcanic track from new 40Ar/39Ar ages on phenocryst phases. Tectonophysics. https://doi.org/10.1016/j.tecto.2012.08.026

Sandwell, D.T., Smith, W.H.F., 2009. Global marine gravity from retracked Geosat and ERS-1 altimetry: Ridge segmentation versus spreading rate. J. Geophys. Res. Solid Earth. https://doi.org/10.1029/2008JB006008

Sclater, J.G., Christie, P.A.F., 1980. Continental stretching: An explanation of the Post-Mid-Cretaceous subsidence of the central North Sea Basin. J. Geophys. Res. Solid Earth 85, 3711–3739. https://doi.org/10.1029/JB085iB07p03711

Seton, M., Müller, R.D., Zahirovic, S., Gaina, C., Torsvik, T., Shephard, G., Talsma, A., Gurnis, M., Turner, M., Maus, S., Chandler, M., 2012. Global continental and ocean basin reconstructions since 200Ma. Earth-Science Rev. https://doi.org/10.1016/j.earscirev.2012.03.002

Smith, A., 1999. The planet beyond the plume hypothesis. Earth-Science Rev. 48, 135–182. https://doi.org/10.1016/S0012-8252(99)00049-5

Souza, K.G., Fontana, R.L., Mascle, J., Macedo, J.M., Mohriak, W.U., Hinz, K., 1993. The southern Brazilian margin: an example of a South Atlantic volcanic margin, in: 3rd International Congress of the Brazilian Geophysical Society.

Steinberger, B., Torsvik, T.H., 2012. A geodynamic model of plumes from the margins of Large Low Shear Velocity Provinces. Geochemistry, Geophys. Geosystems 13, n/a-n/a. https://doi.org/10.1029/2011GC003808

Torsvik, T.H., Amundsen, H., Hartz, E.H., Corfu, F., Kusznir, N., Gaina, C., Doubrovine, P. V., Steinberger, B., Ashwal, L.D., Jamtveit, B., 2013. A Precambrian microcontinent in the Indian Ocean. Nat. Geosci. 6, 223–227. https://doi.org/10.1038/ngeo1736

Torsvik, T.H., Amundsen, H.E.F., Trønnes, R.G., Doubrovine, P. V., Gaina, C., Kusznir, N.J., Steinberger, B., Corfu, F., Ashwal, L.D., Griffin, W.L., Werner, S.C., Jamtveit, B., 2015. Continental crust beneath southeast Iceland. Proc. Natl. Acad. Sci. https://doi.org/10.1073/pnas.1423099112

Torsvik, T.H., Burke, K., Steinberger, B., Webb, S.J., Ashwal, L.D., 2010. Diamonds sampled by plumes from the core–mantle boundary. Nature 466, 352–355. https://doi.org/10.1038/nature09216

Ussami, N., Chaves, C.A.M., Marques, L.S., Ernesto, M., 2013. Origin of the Rio Grande Rise–Walvis Ridge reviewed integrating palaeogeographic reconstruction, isotope geochemistry and flexural modelling. Geol. Soc. London, Spec. Publ. https://doi.org/10.1144/SP369.10

Wilson, J.T., 1965. Submarine fracture zones, aseismic ridges and the International Council of Scientific Unions Line: Proposed Western Margin of the East Pacific Ridge. Nature. https://doi.org/10.1038/207907a0

Wilson, J.T., 1963. Evidence from islands on the spreading of ocean floors. Nature. https://doi.org/10.1038/197536a0

Figure Captions

Figure 1: Regional bathymetric (Amante & Eakins 2009) map, scale in meters, overlain by a shaded-relief display of free-air gravity anomaly, showing the location of RGR and WR and its Tristan-Gough volcanic track (Guyot Province) in the South Atlantic Ocean (SAO), as well as South Atlantic fracture zones (AFFZ: Agulhas-Falkland Fracture Zone; RGFZ: Rio Grande Fracture Zone; RFZ: Romanche Fracture Zone) dividing the SAO in Central, Austral and Falkland segments. The Equatorial segment belongs to the Equatorial Atlantic. The Rio

Grande Rise and Walvis Ridge are located southern of the RGFZ. Paraná-Etendeka Magmatic Provinces are shown in red in the South America and African continents.

Figure 2: RGR focused bathymetric (Amante & Eakins 2009) map, scale in meters overlain by a shaded-relief display of free-air gravity anomaly, which shows the three units of the RGR (Western, Central and Eastern RGR) and surrouding geologic features: Brazilian sedimentary basins (PB: Pelotas Basin; SB: Santos Basin; CB: Campos Basin), São Paulo Plateau, Florianópolis Ridge, Torres High, Jean Charcot Seamounts,Vema Channel, Ponta Grossa Arch and Cruzeiro do Sul Lineament. RGFZ: Rio Grande Fracture Zone. (b) 3D bathymetric (Amante & Eakins 2009) map of the RGR.

Figure 3: (a) Satellite free-air gravity anomaly map, scale in mgal (Sandwell & Smith 2009), overlain by a shaded-relief display of itself and (b) magnetic anomaly map, scale in nT (Meyer et al. 2016), overlain by shaded-relied display of free-air gravity anomaly. Magmatic ages for the RGR, WR and Africa and South America continents are superimposed (ages from Renne et al. 1996; Rohde et al. 2013; O'Connor et al. 2012, 2015; Geraldes et al. 2013; Hoernle et al. 2015) The RGR shows ages between 80 – 87 Ma and 46 Ma.

Figure 4: (a) Map of crustal basement thickness derived from gravity inversion for the RGR, scale in kilometers, with the seismic reflection lines path in black lines (A-B-C-D-E) and yellow circles indicating the location of the seismic Moho depth measurements from Constantino et al. (2017). (b) Crustal cross-section with Moho depth derived from gravity inversion using sediment thickness from seismic interpretation and (c) crustal cross-section with Moho depth from gravity inversion using public domain sediment thickness. The blue line is bathymetry, the green line is top basement, the red line is the Moho calculated from gravity inversion and yellow circles are the location of the Moho from seismic interpretation

from Constantino et al. (2017). (d) Cross-plot comparing gravity Moho depths with Moho depths from seismic reflection (from Constantino et al. 2017).

Figure 5: Map of crustal basement thickness derived from gravity inversion with superimposed shaded relief free-air gravity anomaly for the South Atlantic Ocean showing anomalous thick crust for RGR and WR. Magmatic ages are are shown (ages from Renne et al. 1996; Rohde et al. 2013; O'Connor et al. 2012, 2015; Geraldes et al. 2013; Hoernle et al. 2015). The RGR shows ages between 80 – 87 Ma and 46 Ma. The conjugate WR ages are shown in the 87 – 107 Ma segment of WR.

Figure 6: (a) Map of crustal basement thickness for the RGR with scale in kilometers. Shaded relief free-air gravity is superimposed. (b-d) Three crustal-scale cross-sections with Moho depth extracted from the results of the gravity inversion. Cross-section locations are shown in (a). CNS: Cretaceous Normal Superchron.

Figure 7: Plate reconstruction using GPlates 1.5 of magnetic anomalies and crustal thickness from gravity inversion (with superimposed shaded relief free air gravity) for the S. Atlantic for ages of 90, 80 and 70 Ma. The reconstructions at 80 Ma show magnetic anomaly C34 on the divergent plate boundary and RGR and WR as a single body located at that divergent plate boundary.

Figure 8: (a) Plate reconstructions using Gplates 1.5 of crustal thickness from gravity inversion (with superimposed shaded relief free-air gravity) at 83 Ma showing RGR and WR forming a single body located at the divergent plate boundary. (b) Crustal cross-sections with Moho from gravity inversion and magnetic anomaly for a profile restored to 83 Ma running across Western RGR, Central RGR and WR.

Figure 9: Plate reconstruction, using Gplates 1.5, of crustal thickness from gravity inversion (with superimposed shaded relief free-air gravity) for the S. Atlantic from 70 to 40 Ma at 10 Myr intervals.

Figure 10: (a) Plate reconstruction, using Gplates 1.5, of crustal thickness from gravity inversion (with shaded relief free-air gravity) at 54 Ma. (b) Crustal cross-sections with Moho from gravity inversion along the axes of the Eastern RGR and WR. Line locations are shown in (a).

Figure 11: Plate reconstruction, using GPlates 1.5, of crustal thickness from gravity inversion (with superimposed shaded relief free-air gravity) at 50 Ma. Past sea-floor spreading axes are shown and indicate successive eastward migration and jumps of sea-floor spreading ridge axes which lead to the separation of the Western, Central and Eastern RGR and WR.

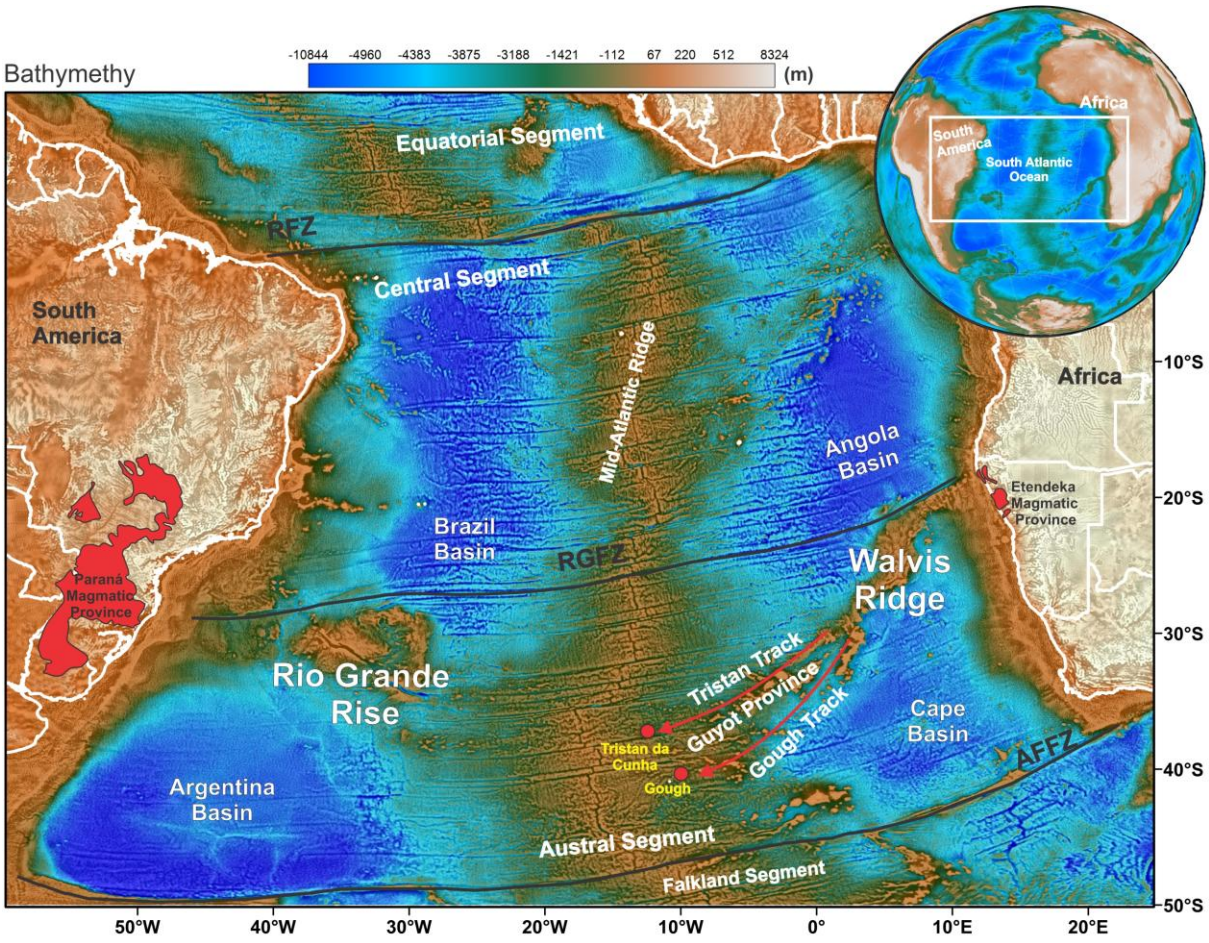
Bathymethy
-10844 -4960 -4383 -3875 -3188 -1421 -112 67 220 512 8324
(m)
Africa
South America
South Atlantic Ocean
Equatorial Segment
RFZ
Central Segment
South America
Mid-Atlantic Ridge
Africa
Angola Basin
Etendeka Magmatic Province
Brazil Basin
RGFZ
Walvis Ridge
Paraná Magmatic Province
Rio Grande Rise
Tristan Track
Guyot Province
Gough Track
Cape Basin
Tristan da Cunha
Gough
AFFZ
Argentina Basin
Austral Segment
Falkland Segment
10°S
20°S
30°S
40°S
50°S
50°W
40°W
30°W
20°W
10°W
0°
10°E
20°E

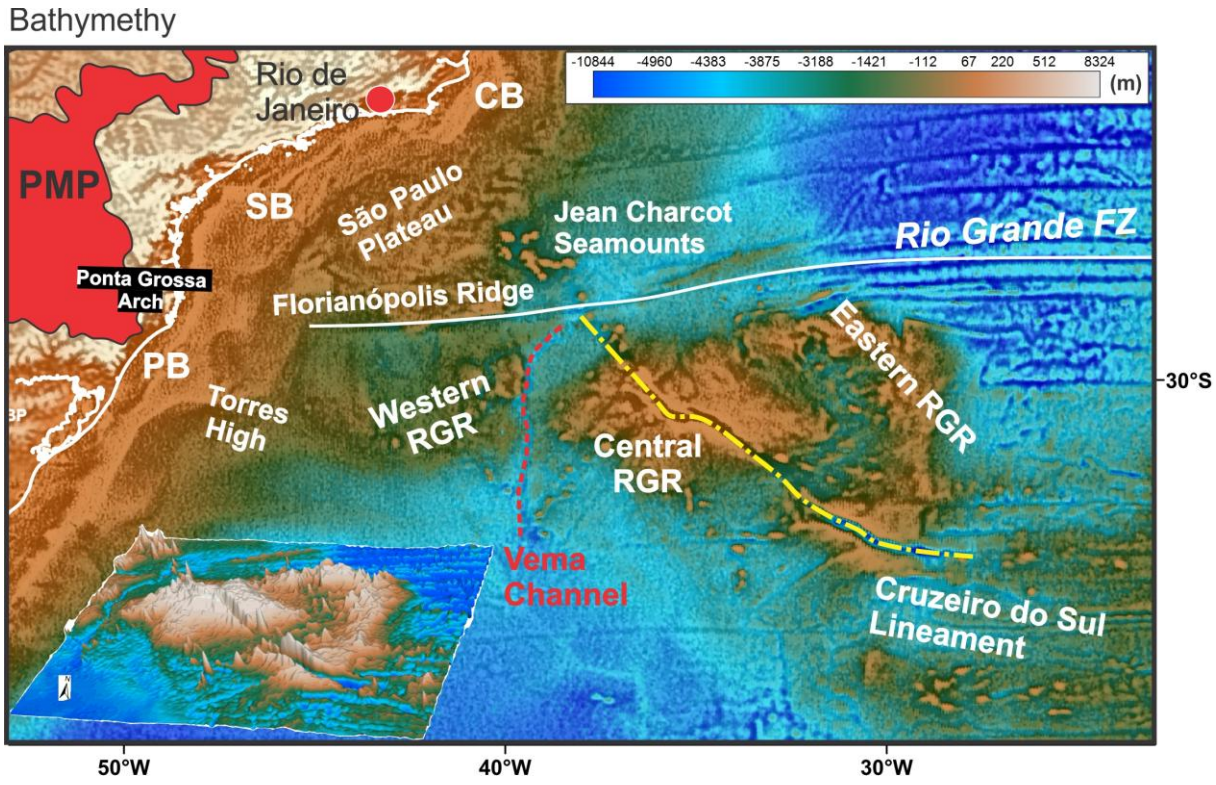
Bathymethy
-10844 -4960 -4383 -3875 -3188 -1421 -112 67 220 512 8324
(m)
Rio de Janeiro
CB
PMP
SB
São Paulo Plateau
Jean Charcot Seamounts
Rio Grande FZ
Ponta Grossa Arch
Florianópolis Ridge
PB
Torres High
Western RGR
Central RGR
Eastern RGR
Vema Channel
Cruzeiro do Sul Lineament
30°S
50°W
40°W
30°W

Free-air gravity anomaly map

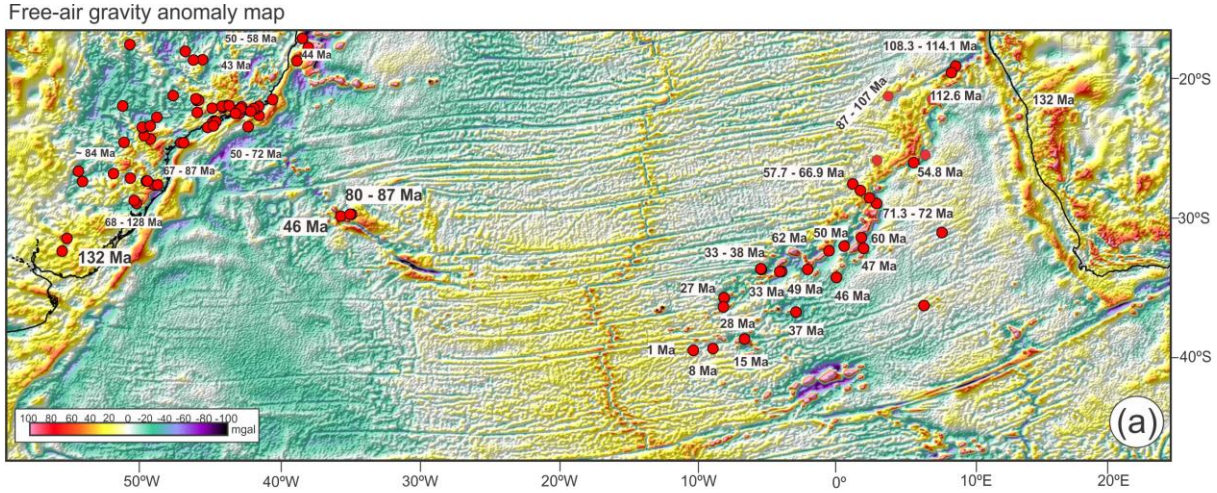

EMAG2v3: Earth Magnetic Anomaly map

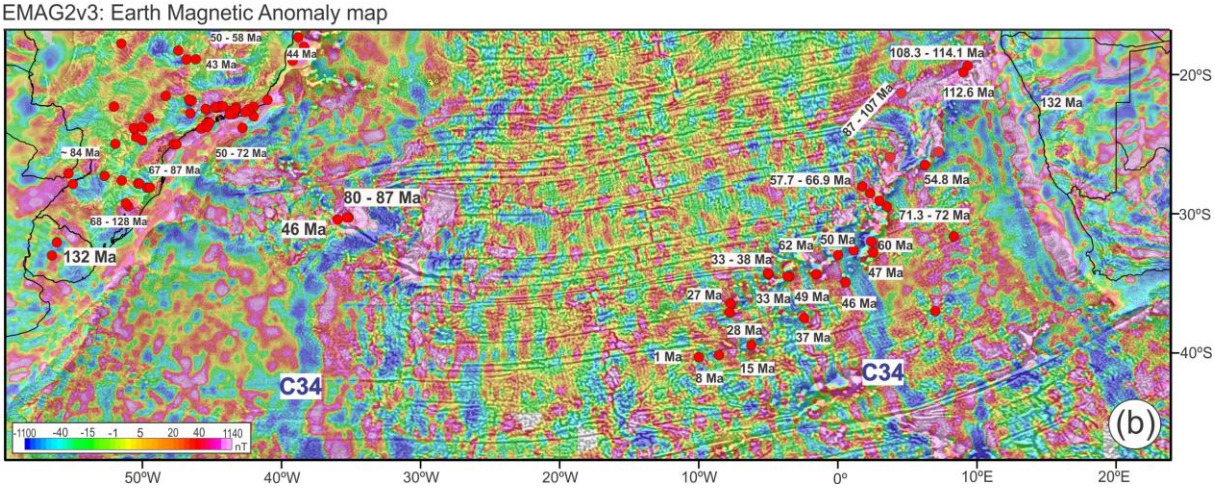

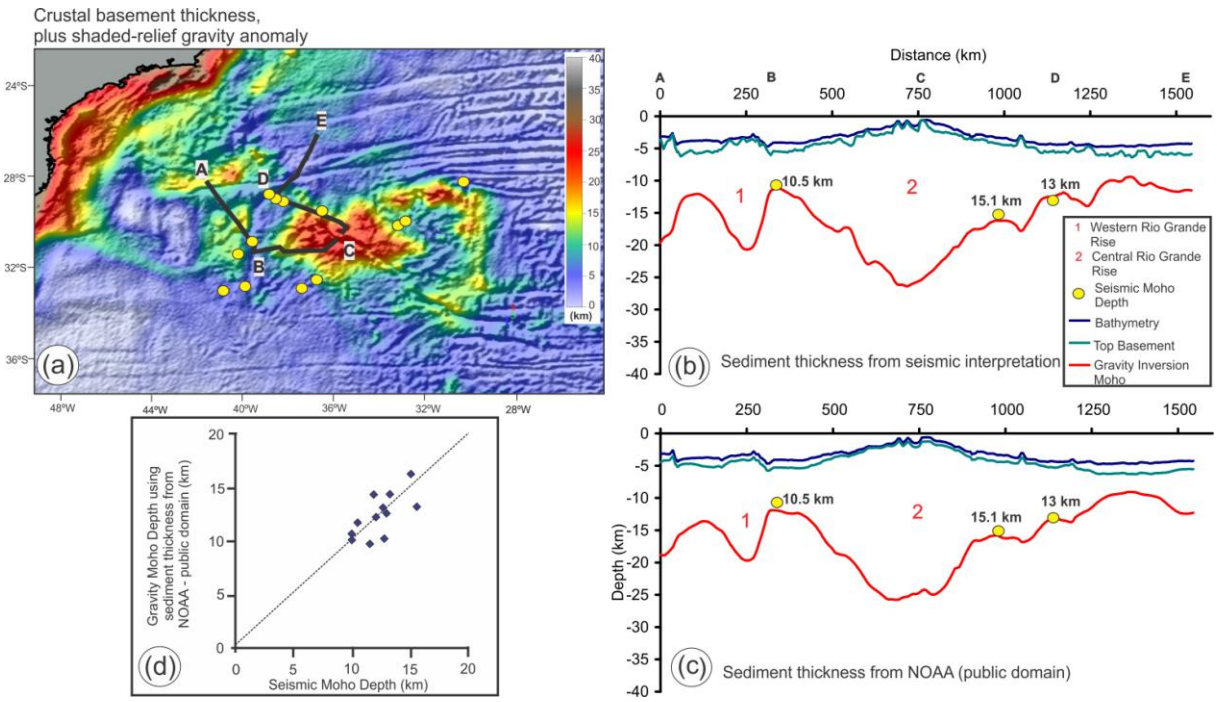
Crustal basement thickness,
plus shaded-relief gravity anomaly
24°S
28°S
32°S
36°S
48°W
44°W
40°W
36°W
32°W
28°W
A
B
C
D
E
(km)
(a)
Distance (km)
0
250
500
750
1000
1250
1500
10.5 km
15.1 km
13 km
1
2
1 Western Rio Grande Rise
2 Central Rio Grande Rise
Seismic Moho Depth
Bathymetry
Top Basement
Gravity Inversion Moho
(b)
Sediment thickness from seismic interpretation
Depth (km)
(c)
Sediment thickness from NOAA (public domain)
Gravity Moho Depth using sediment thickness from NOAA - public domain (km)
Seismic Moho Depth (km)
(d)

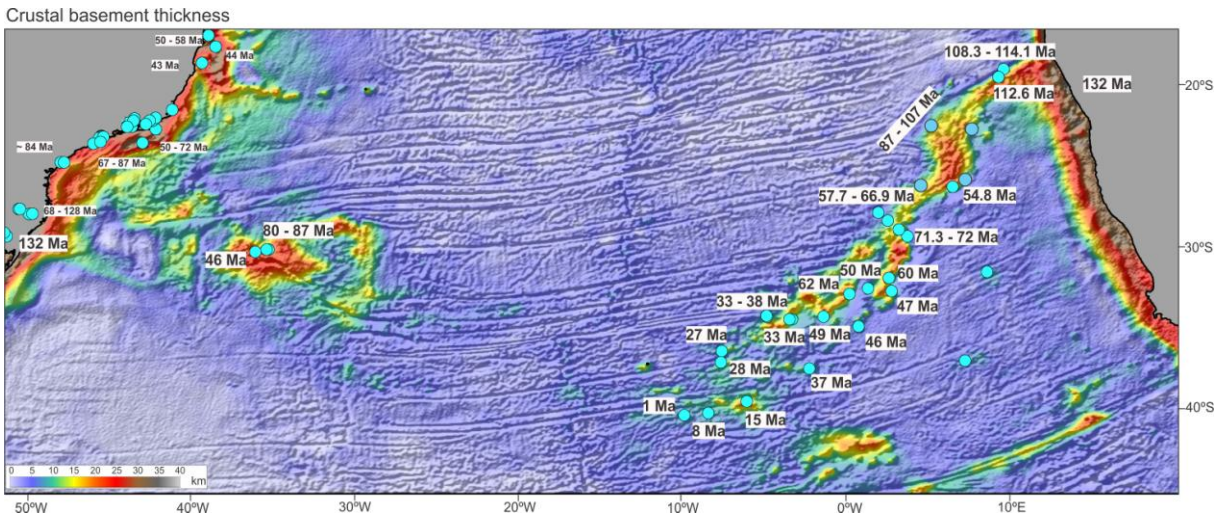
Crustal basement thickness
50 - 58 Ma
44 Ma
43 Ma
~ 84 Ma
50 - 72 Ma
67 - 87 Ma
68 - 128 Ma
132 Ma
80 - 87 Ma
46 Ma
108.3 - 114.1 Ma
112.6 Ma
132 Ma
87 - 107 Ma
57.7 - 66.9 Ma
54.8 Ma
71.3 - 72 Ma
50 Ma
60 Ma
62 Ma
47 Ma
33 - 38 Ma
27 Ma
33 Ma
49 Ma
46 Ma
28 Ma
37 Ma
1 Ma
15 Ma
8 Ma
0 5 10 15 20 25 30 35 40
km
50°W
40°W
30°W
20°W
10°W
0°W
10°E
20°S
30°S
40°S

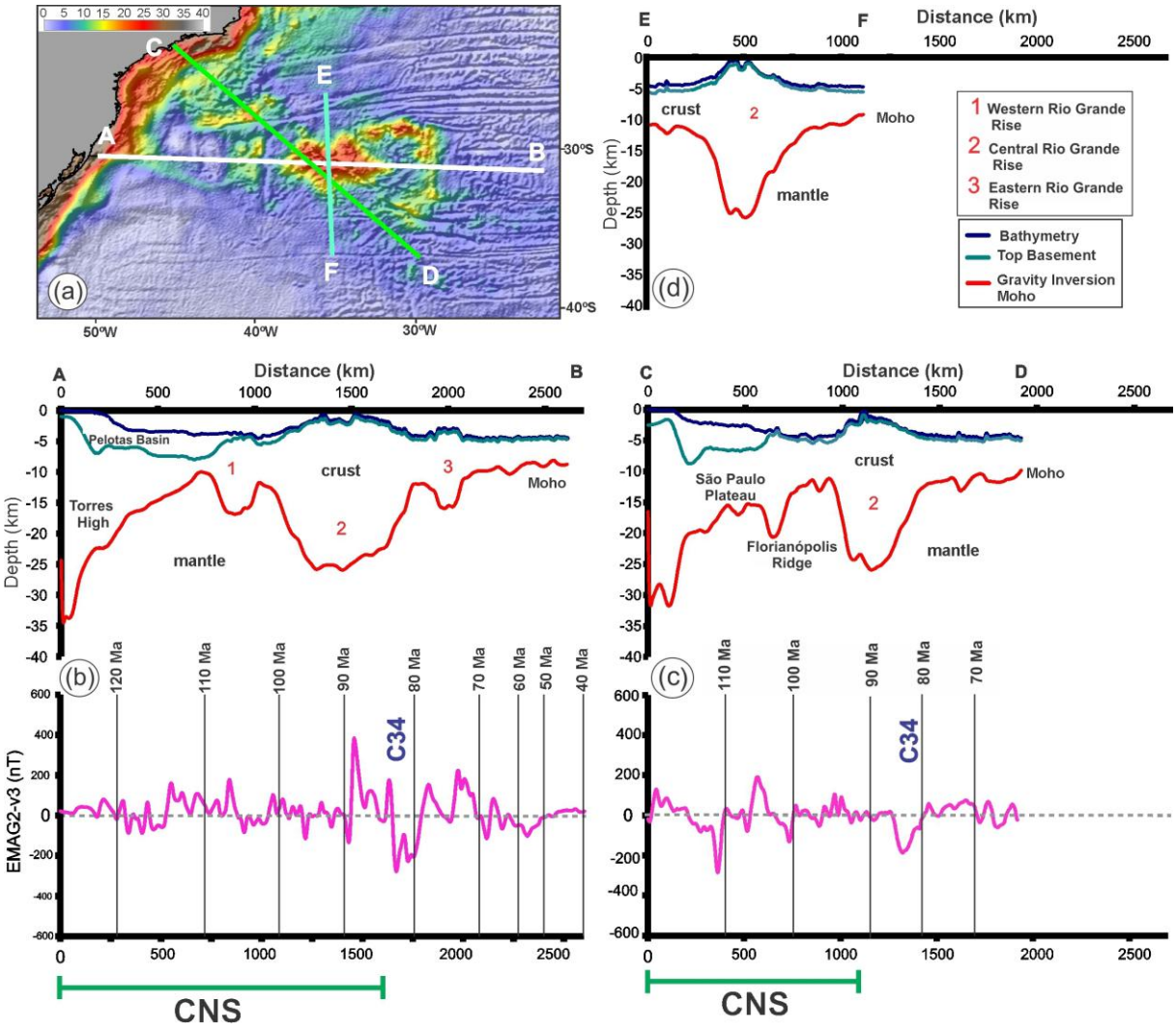
0 5 10 15 20 25 30 35 40
C
E
A
B
F
D
(a)
50°W
40°W
30°W
30°S
40°S
E
F
Distance (km)
0 500 1000 1500 2000 2500
crust
2
Moho
mantle
Depth (km)
(d)
1 Western Rio Grande Rise
2 Central Rio Grande Rise
3 Eastern Rio Grande Rise
Bathymetry
Top Basement
Gravity Inversion Moho
A
B
Distance (km)
Pelotas Basin
1
crust
3
Moho
Torres High
2
mantle
Depth (km)
(b)
120 Ma
110 Ma
100 Ma
90 Ma
80 Ma
70 Ma
60 Ma
50 Ma
40 Ma
C34
EMAG2-v3 (nT)
CNS
C
D
Distance (km)
crust
São Paulo Plateau
Moho
2
Florianópolis Ridge
mantle
(c)
110 Ma
100 Ma
90 Ma
80 Ma
70 Ma
C34
CNS

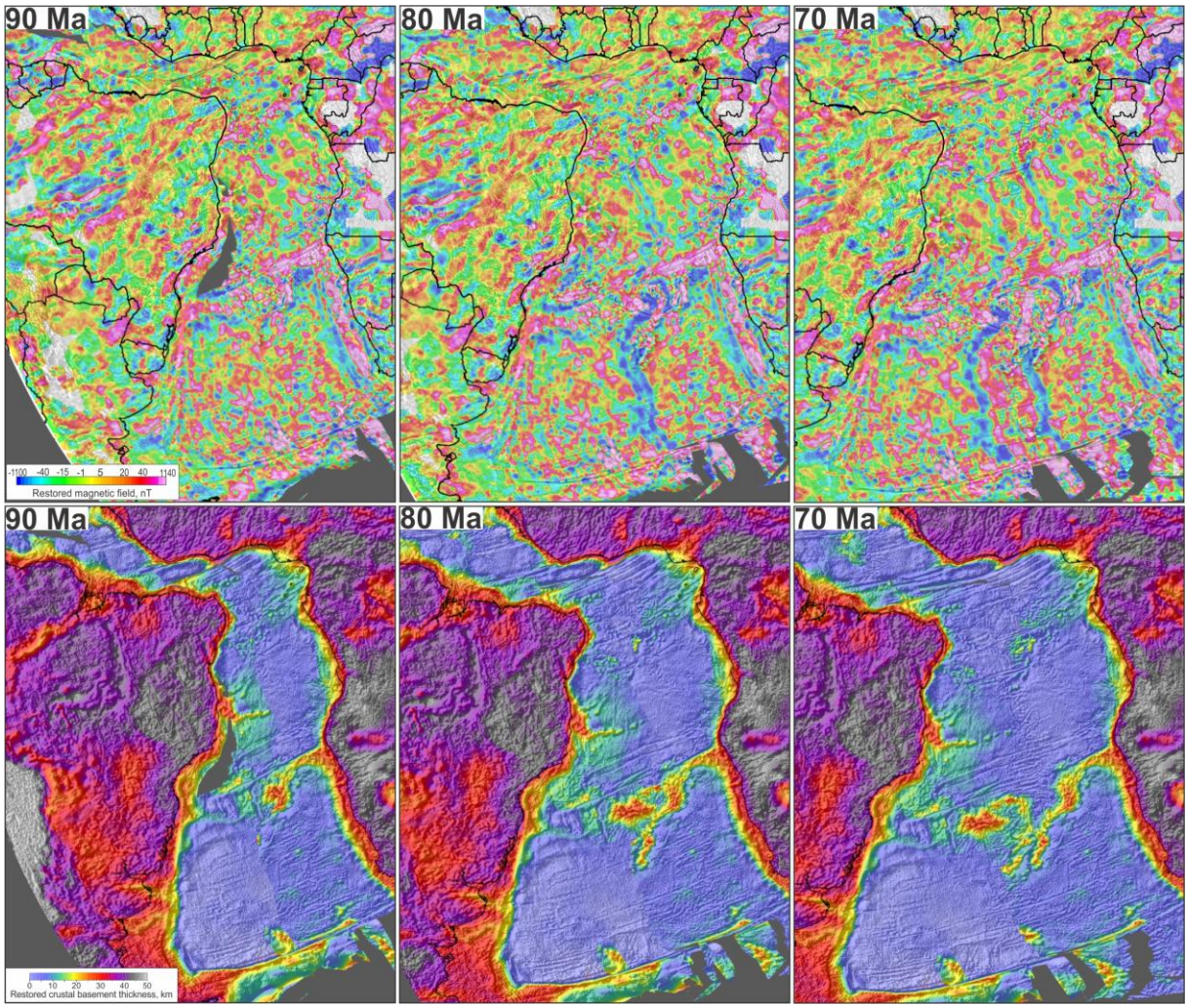
90 Ma
80 Ma
70 Ma
-1100 -40 -15 -1 5 20 40 1140
Restored magnetic field, nT
90 Ma
80 Ma
70 Ma
0 10 20 30 40 50
Restored crustal basement thickness, km

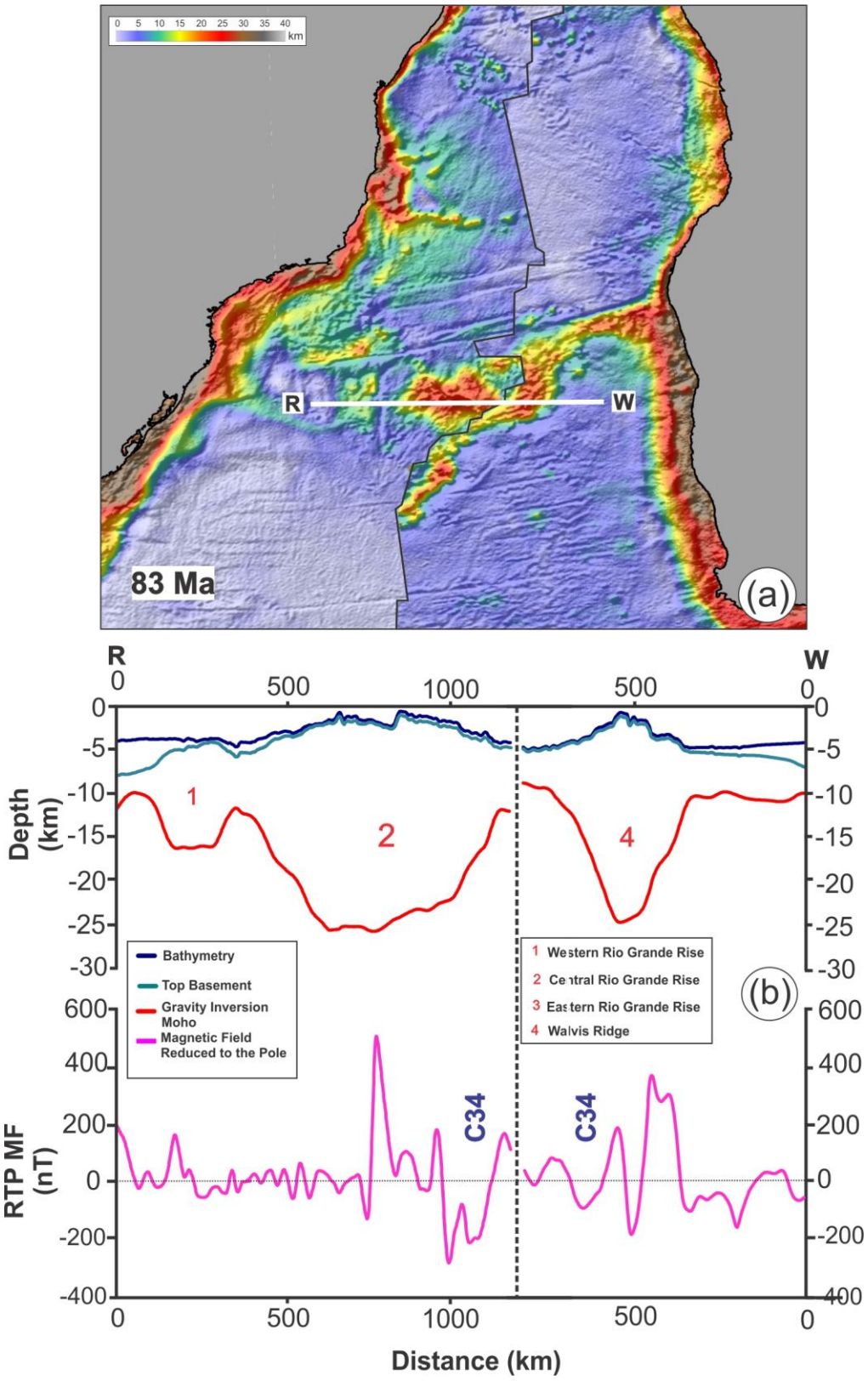
0 5 10 15 20 25 30 35 40
km
R
W
83 Ma
(a)
R
W
0
500
1000
500
0
Depth (km)
0
-5
-10
-15
-20
-25
-30
1
2
4
Bathymetry
Top Basement
Gravity Inversion Moho
Magnetic Field Reduced to the Pole
1 Western Rio Grande Rise
2 Central Rio Grande Rise
3 Eastern Rio Grande Rise
4 Walvis Ridge
(b)
600
400
200
0
-200
-400
RTP MF (nT)
C34
C34
Distance (km)

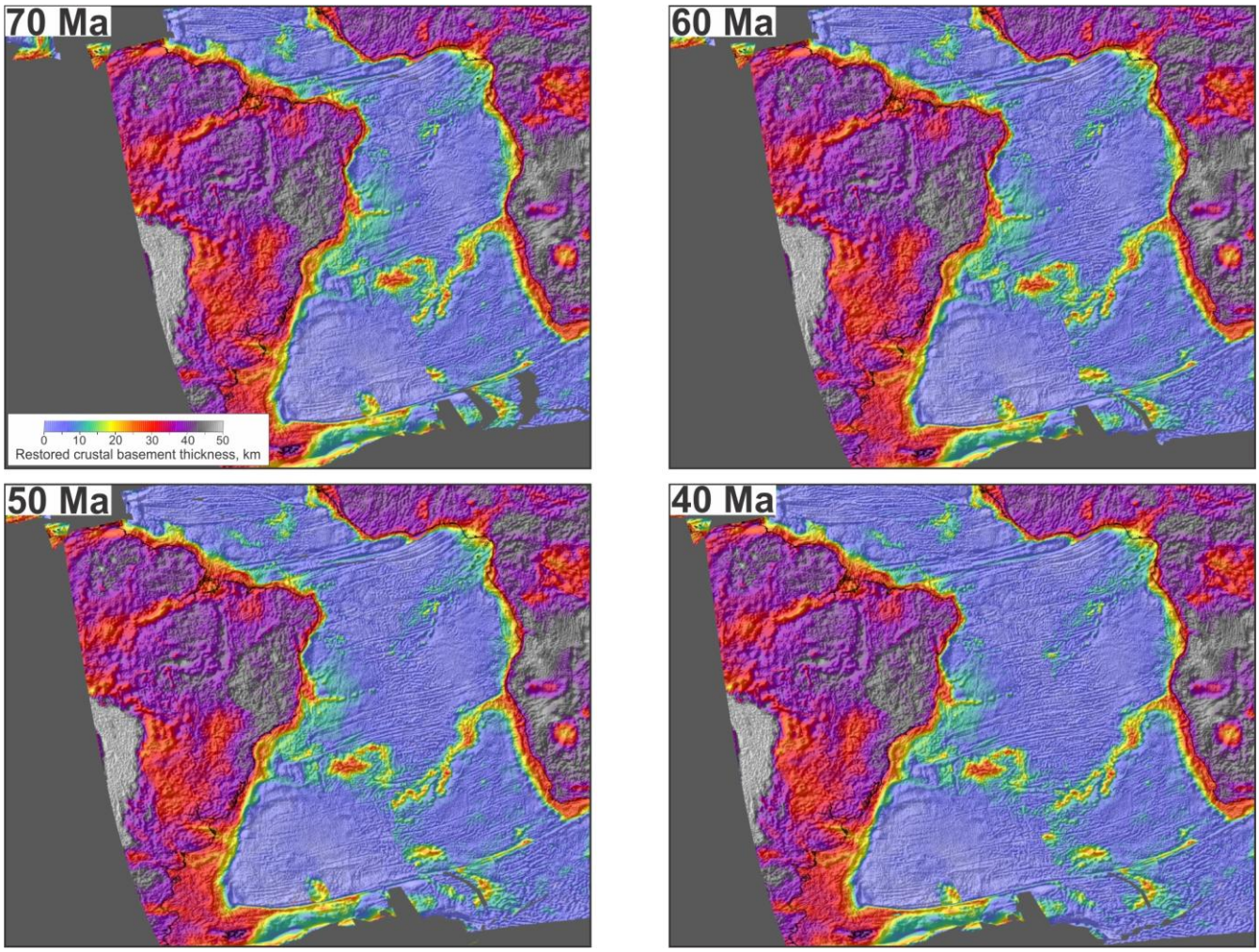
70 Ma
60 Ma
50 Ma
40 Ma
0 10 20 30 40 50
Restored crustal basement thickness, km

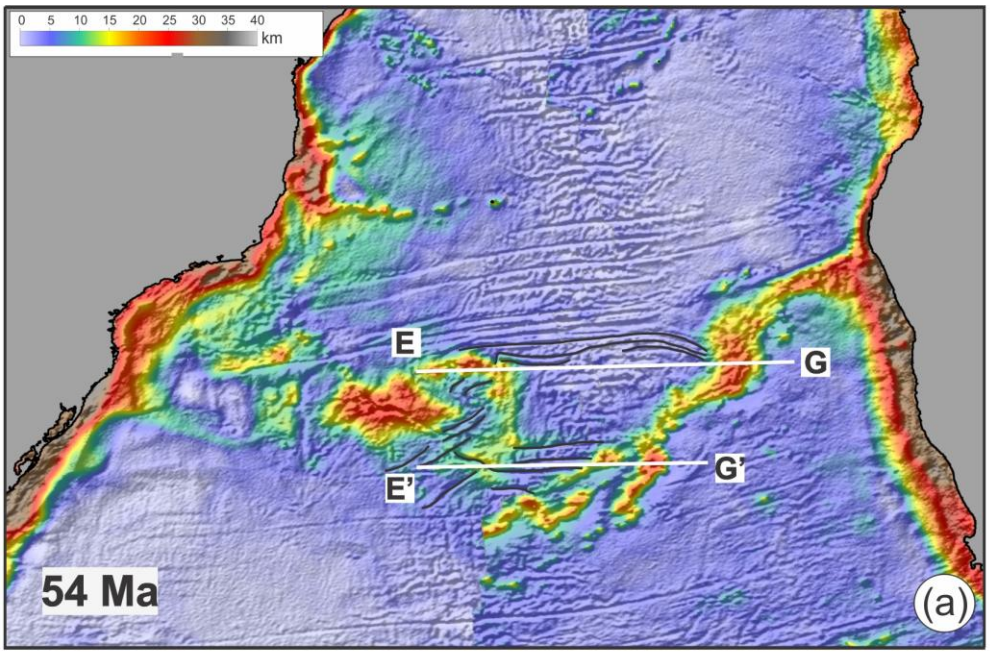
0 5 10 15 20 25 30 35 40
km
E
G
E'
G'
54 Ma
(a)

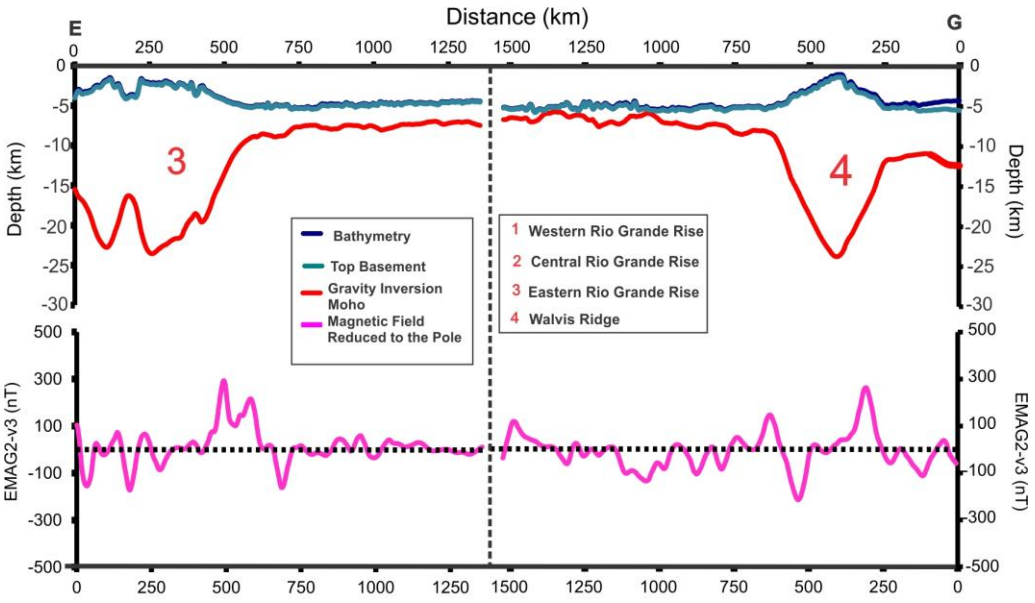
E
G
Distance (km)
Depth (km)
EMAG2-v3 (nT)
3
4
Bathymetry
Top Basement
Gravity Inversion Moho
Magnetic Field Reduced to the Pole
1 Western Rio Grande Rise
2 Central Rio Grande Rise
3 Eastern Rio Grande Rise
4 Walvis Ridge

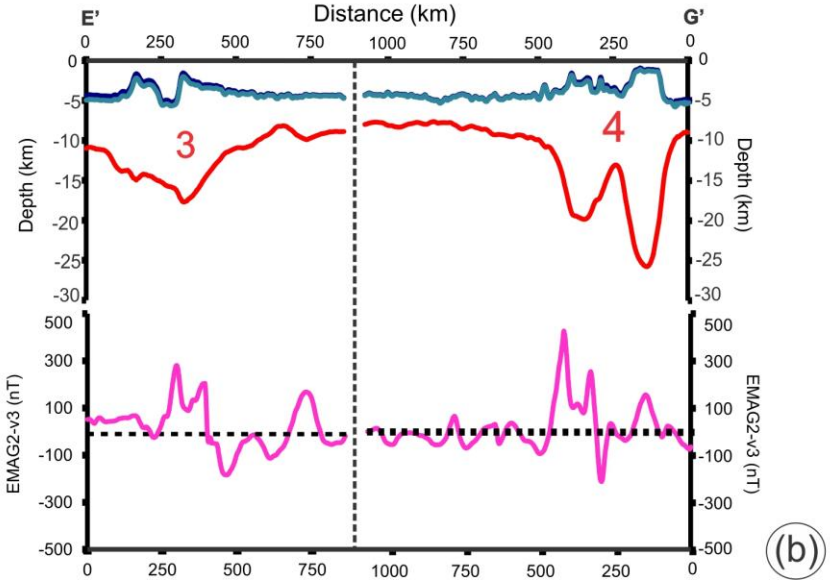
E'
G'
Distance (km)
Depth (km)
EMAG2-v3 (nT)
3
4
(b)

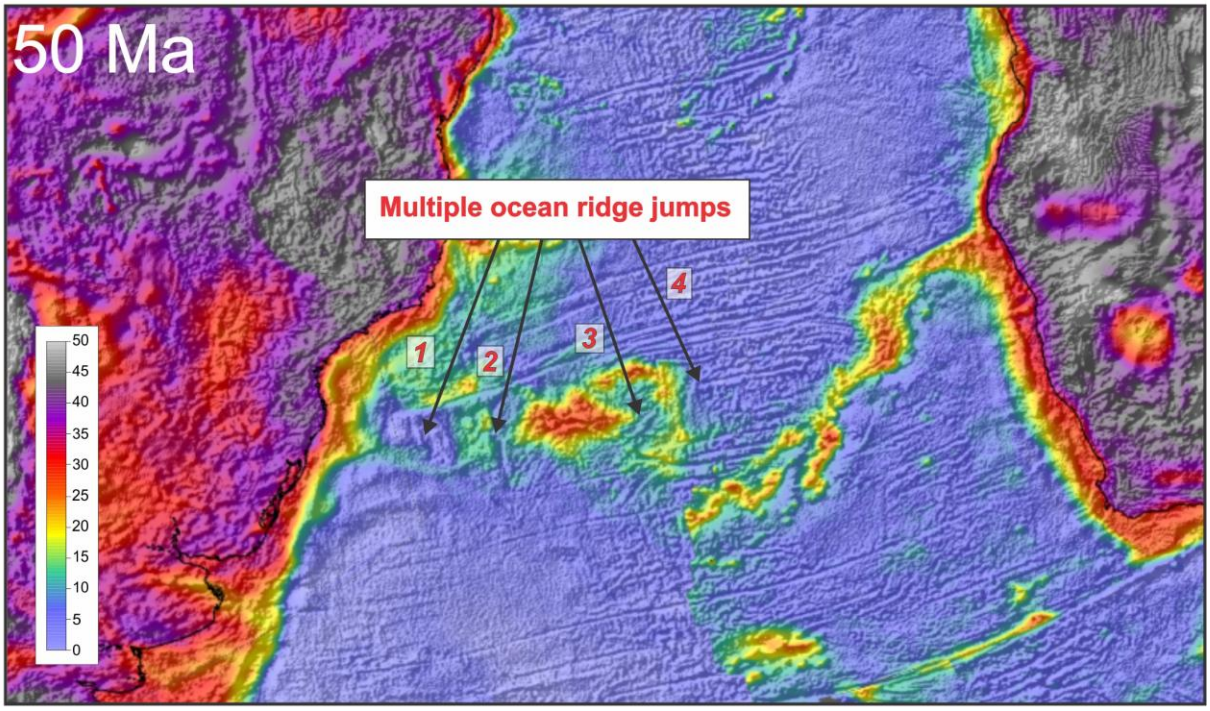
50 Ma
Multiple ocean ridge jumps
1
2
3
4
50
45
40
35
30
25
20
15
10
5
0